ENERGY DISTRIBUTION FOR SH-WAVES IN SLIGHTLY ANISOTROPIC MATERIALS

R.B. Mignogna, P.P. Delsanto* and A.V. Clark**

Nondestructive Evaluation Section, Code 6385
Naval Research Laboratory
Washington, DC 20375-5000

ABSTRACT

Many polycrystalline metal aggregates display a slight amount of anisotropy due to texture that develops during fabrication procedures such as rolling. This macroscopic anisotropy produces a birefringence of SH-waves propagating normal to the plate, i.e., the velocity of SH-waves polarized parallel to the rolling direction is usually faster than that of SH-waves polarized perpendicular to the rolling direction. For polarization angles not in or perpendicular to the rolling direction the wave is assumed to split into two waves, one polarized parallel and one polarized perpendicular to the rolling (similar to what is observed for particular propagation directions in single crystals). However slightly anisotropic materials have only a small percentage of preferential grain alignment, the bulk of the grains being of random orientation. In consideration of these materials being nearly isotropic, having slight anisotropy superimposed, and the possibility of multiple textures, we address the energy distribution of SH-waves as a function of polarization angle with respect to the material symmetry axes and the transducer orientation. The importance of considering attenuation in this work is also addressed.

INTRODUCTION

The work presented in this paper is the result of a number of observations made during our study of acoustoelasticity and texture. Anomalies were noted while observing amplitude and arrival times of echoes as a function of transducer polarization direction. Most of these 'anomalies' were at first attributed to experimental error due to working with contact transducers. However, further consideration of the possible effects of texture variations in polycrystalline materials indicated that these observation may merit further investigation.

Assuming a material to be homogeneous and knowing the elastic constants for the material, wave speeds and propagation directions can be calculated using Kristoffels equation. For materials assumed to be truly isotropic and homogeneous it is found that both longitudinal and shear waves are directionally independent. That is, if a horizontally polarized SH-wave was generated propagating parallel to the normal of a plate (or any arbitrary direction) the wave speed would be the same for all polarization directions. Anisotropic single crystals may display directional dependence. Two simple examples are propagation of SH-waves along the [001] and

*Dip. Fisica del Politecnico, Torino, Italy
**Fracture and Deformation Div., NBS, Boulder, CO 80303

[011] directions of cubic materials. SH-waves are isotropic when propagating along the [001] direction, i. e. independent of polarization direction. However, SH-waves propagating along the [011] direction are dependent upon the polarization direction. Two SH-wave speeds exist in this direction, one for waves polarized in the [100] direction and another for waves polarized in the [0$\bar{1}$1] direction. Attempts to generate waves polarized at arbitrary directions will produce two waves, one polarized in the [100] and the other polarized in the [0$\bar{1}$1] direction. This is easily observed in a large single crystal (approximately 2 cm path length for aluminum) using the pulse-echo technique. SH-waves generated with polarization directions along either of the two principal polarization directions produce a single pulse-echo pattern. However, as the transducer is rotated toward the other principal direction a second distinct pulse-echo pattern arises, grows in amplitude as the transducer is rotated while the original diminishes, extinguishing completely after a rotation of 90 degrees. In all cases mentioned the energy vector is parallel to the wave normal.

If the grain orientation for a polycrystalline material is totally random the material would be, on a macroscopic scale, isotropic. Many polycrystalline materials display some degree of anisotropy to due to preferred grain orientation (texture). If a polycrystalline material displays isotropic symmetry with respect to normally incident SH-waves at what point or degree of preferred grain orientation will the material display a measurable degree of anisotropy with respect to SH-waves? We are discussing a macroscopic anisotropy of an aggregate material that can be treated as a perturbation of the isotropic case and not anisotropy due to the lattice structure in a single crystal.

If the polarization direction in the material remains parallel to the transducer polarization direction for isotropic materials but is directionally dependent for anisotropic materials is it possible to observe part of the transmitted energy having its polarization direction remain parallel to the transducer, at arbitrary angles with respect to the symmetry directions for slightly anisotropic materials? Most rolled polycrystalline metals have texture variations in both degree and type. For rolled plates, the variations usually occur in a 'layered' manner and are symmetric about the mid-plane. By degree we mean the 'number' of oriented grains and by type, the preferred direction of the oriented grains. These variations being dependent on the material, alloying elements, fabrication and thermal histories. With this in mind, can effects of 'secondary' textures be observed during rotation of an SH-wave transducer?

This paper presents experimental results from measurements in rolled plate materials of normal incidence SH-waves as a function of polarization angle. Discussion is included considering the possible effects of both slight anisotropy and a layered or inhomogeneous texture through the thickness.

CONSIDERATION OF THE AGGREGATE MATERIAL

Papadakis[1] discussed the possibility of 'constructing' any type of symmetry desired from polycrystalline materials by using controlled texturing and sectioning of the material. At present we are interested in making stress and texture measurements on materials that are currently being used commercially. Instead of designing texture it is necessary to assess the texture.

Questions arise in the area of what assumptions can be or need to be made for SH-wave measurements in polycrystalline materials. Let us first consider that on a macroscopic scale a rolled plate displays orthotropic symmetry. In many cases, a more accurate description would be that the plate displays two 2-fold symmetry axes in the plane of the plate (parallel and perpendicular to the rolling direction) but is inhomogeneous along the plate normal due to texture variations through the thickness (however, symmetric about the mid plane). We also assume the SH-wave velocity is slightly different for waves polarized parallel versus waves polarized perpendicular to the rolling direction. As this is a polycrystalline aggregate, is the attenuation (energy loss) of the wave necessarily the same parallel and perpendicular to rolling direction? Does the wave split equally between the two symmetry axis? What is the effect of multiple textures in view of a 'layered' texture structure in rolled plates?

Two types of measurement schemes were used; one incorporating a single SH-wave transducer in a pulse-echo mode and the second incorporated two SH-wave transducers in a pitch-catch mode. For discussion of these measurements let the X_1 axis be perpendicular and the X_2 axis be parallel to the rolling direction of the plate. We also define the angle θ to be the angle between the X_1 axis and the transmitter polarization direction and the angle ϕ to be the angle between the X_1 axis and the receiver polarization direction. In the case of pulse echo measurements, $\phi = 0°$.

For slightly anisotropic materials, the birefringence is usually defined as $B_0 = (V_2 - V_1)/V_0$ where V_1 and V_2 are the velocity of normal incidence SH-waves polarized parallel to the X_1 and X_2, respectively and $V_0 = (V_1 + V_{2)}/2$. We will first consider only the usual birefringence, i.e. splitting of the wave parallel and perpendicular to the rolling direction, for pule-echo measurements in slightly anisotropic materials. The displacement of an SH-wave, as viewed by a transducer at an arbitrary angle with respect to the X_1 axis, can be written in terms of the angular frequency, ω, time, t, wave numbers, k_i, thickness, d, echo number, n, and attenuations, α_i, as

$$u = e^{-i\omega t} [G_1 e^{-a_1} \cos^2 \theta e^{iK_1} + G_2 e^{-a_2} \sin^2 \theta e^{iK_2}] \tag{1}$$

where $K_i = 2\text{ndk}_i$ and the energy loss (including attenuation, grain scattering and transducer losses such as coupling) $a_i \propto 2\text{nd}\ \alpha_i$. As we are dealing with polycrystalline aggregates, we have allowed for the possibility that the energy loss is not equal for wave polarized along the rolling and transverse directions. By the same reasoning, the coefficients G_i allow for the possibility that the wave does not split by geometric factors alone into two components.

The wave number, k_1, can be written as a function of the birefringence, B_0,

$$k_1 = \omega/V_1 = \omega/[V_0(1 - B_0/2)] \approx k_0 (1 + B_0/2)$$

where $k_0 = \omega/V_0$ and neglecting terms of order $(B_0/2)^2$ and higher. Similarly, k_2 can be written as

$$k_2 \approx k_0 (1 - B_0/2)$$

By writing the displacement in polar form we have both the resultant amplitude and phase of the received signal, where the resultant amplitude, R', can be written as

$$R' = [Z'^2_1 + Z'^2_2 + 2Z'_1 Z'_2 \cos (K_1 - K_2)]^{1/2} \tag{2}$$

and phase, γ', as

$$\gamma' = \tan^{-1} [(Z'_1 \sin K_1 + Z'_2 \sin K_2)/(Z'_1 \cos K_1 + Z'_2 \cos K_2)] \tag{3}$$

where

$$Z'_1 = G_1 e^{-a_1} \cos^2 \theta$$

and

$$Z'_2 = G_2 e^{-a_2} \sin^2 \theta$$

The primes (') are used to distinguish the pulse-echo from the pitch-catch case.

Assuming geometric splitting of the wave along the X_1 and X_2 axis with $G_1 = G_2 = 1$, and equal attenuation, $a_1 = a_2$, we find that the maximum interference due to birefringence occurs at 45° for all values of the birefringence and for any echo. However, if the attenuation of the wave polarized parallel to the X_1 direction is different from the wave polarized parallel to the X_2 direction, the angle at which maximum interference occurs varies with respect to echo number,

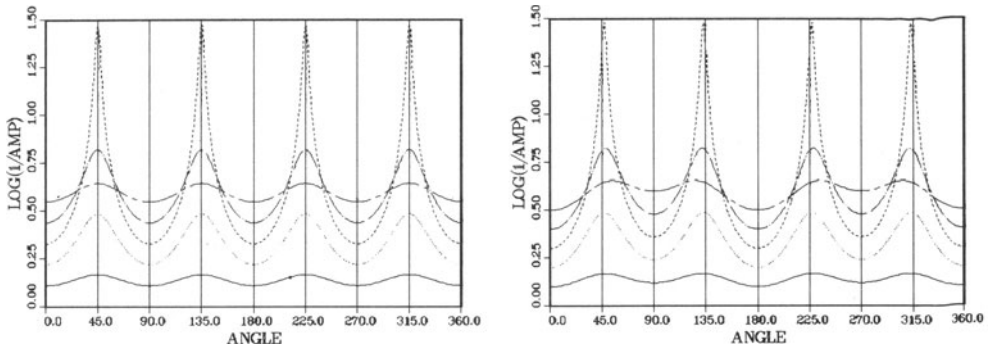

Fig. 1. Log of inverse amplitude as a function of angle for pulse-echo technique, $B_0 = 0.0035$. Curve generated from eq. 4: echo 1# —, #2 . . ., #3 ---- #4 $-\cdot-\cdot-$, #5 ——— (a) $a1 = a2 = 0.11$, maximum interference occurs at 45°. (b) $a1 = 0.10$, $a2 = 0.12$, maximum interference occurs at; $\theta =$ 48°, 47°, 47°, 48°, and 54° for echo #1 through 5, respectively.

birefringence and difference in the attenuations. Examples of the effects of equal and unequal attenuation for the same birefringence are shown in Fig. 1a and 1b, respectively. These perturbations on the angle and amplitude, due to unequal attenuation, may introduce errors in stress measurement techniques that utilize the maximum interference, such as the technique described by Iwashimizu and Kubomura[4]. However, SH-wave speed measurements for polarization directions parallel to the X_1 and X_2 directions are not effected by unequal attenuation.

In an attempt to gain more insight into how the SH-wave splits due to texture in a polycrystalline material, a two transducer pitch-catch arrangement was used. With this arrangement the receiver angle can be set independently of the transmitter. The displacement, as seen by the receiving transducer can be written as

$$u = e^{-i\omega t}\,[G_1\, e^{-a_1} \cos\theta \cos\phi\, e^{iK_1} + G_2\, e^{-a_2} \sin\theta \sin\phi\, e^{iK_2}] \tag{4}$$

In this case the echo numbers, n, are not integers, but will have values $1/2, 1-1/2, 2-1/2, \ldots n-1/2$ (the first signal detected by the receiver has traveled only 1/2 round trip). The amplitude, R, and phase, γ, will be

$$R = [Z_1^2 + Z_2^2 + 2Z_1 \cos(K_1 - K_2)]^{1/2} \tag{5}$$

and

$$\gamma = \tan^{-1}[(Z_1 \sin K_1 + Z_2 \sin K_2)/(Z_1 \cos K_1 + Z_2\, cost\, K_2)] \tag{6}$$

where

$$Z_1 = G_1\, e^{-a_1} \cos\theta \cos\phi$$

and

$$Z_2 = G_2\, e^{-a_2} \sin\theta \sin\phi$$

Similar effects due to unequal attenuation, as shown for the pulse echo case, occur for the two transducer pitch-catch case. For pulse echo measurements, $Z'_1 = 0$ when $\theta = 90°$ and $Z'_2 = 0$ when $\theta = 0°$. In both cases, when the transducer polarization direction is oriented along one of the axes, the phase is a linear function of the echo number. Similarly, for pitch catch measurements, $Z_1 = 0$ when $\theta = 90°$ or $\phi = 90°$ and $Z_2 = 0$ when $\theta = 0°$ or $\phi = 0°$. For the pitch-catch case, if either the transmitter or receiver is oriented along one of the axes, the phase is a linear function of the echo number.

However, unequal attenuation does not effect the arrival time of subsequent echoes (for SH-waves polarized parallel or perpendicular to the rolling direction) nor does it modify the echo train envelope to the extent and manner that is observed (Figs. 2a, 3a, 4a, 5a and 5b). It must be noted that these effects are observable but are 'small' in comparison to the effect of the dominant symmetry in the plane of the plate. One way to account for the observed effects is to assume another wave component is incident upon the receiver. Possible physical causes could be some form of scattering, secondary texture or layered texture. As a first 'guess' we will add one additional component to eq. 4 and define it in a similar fashion as we have for the birefringence. We will assume an amplitude having the form

$$u = e^{-i\omega t}\,[(G_1\, e^{-a_1} \cos\theta\, cost\ \phi\, e^{iK_1} + G_2\, e^{-a_2} \sin\theta \sin\phi\, e^{iK_2})$$

$$+ G_3\, e^{-a_3} \cos(\theta - \phi)\, e^{iK_3}] \tag{7}$$

where

$$K_3 = 2ndk_3 = 2ndk_0\,[1 + f(\theta)].$$

We are also assuming that $f(\theta)$ is of the same order of magnitude as the birefringence. A possible function may be of the form

$$f(\theta) = (B_0 \cos 2\,\theta)/2$$

such that $k_3 = k_1$ for $\theta = 0°$ and $k_3 = k_2$ for $\theta = 90°$. The subscript '3' is not related to an axis of the plate but merely denotes the extra components. G_3 is the relative amplitude (where we will set $G_1 = G_2$ and $G_1 + G_3 = 1$ for all of the following discussion), a_3 is related to the attenuation and $\cos(\theta - \phi)$ is an angular dependence for this component. The resultant amplitude can be written

$$R = [Z_1^2 + Z_2^2 + Z_3^2 + 2Z_1 Z_2 \cos(K_1 - K_2) + 2Z_1 Z_3 \cos(K_1 - K_3)$$

$$+ 2Z_2 Z_3 \cos(K_2 - K_3)]^{1/2} \tag{8}$$

and the phase

$$\gamma = \tan^{-1}\,[Z_1 \sin K_1 + Z_2 \sin K_2 + Z_3 \sin K_3)/(Z_1 \cos K_1 + Z_2 \cos K_2 + Z_3 \cos K_3)] \tag{9}$$

where Z_1 and Z_2 remain the same as defined previously

$$Z_3 = G_3\, e^{-a_3} \cos(\theta - \phi).$$

Figure 2a presents amplitude data versus echo number using the pitch-catch technique on 2024-T351 aluminum. The transmitter polarization direction was 45° ($\theta = 45°$) and the receiver polarization was 315° ($\phi = 315°$). Electromagnetic acoustic transducers (EMATs) were used for both the transmitter and receiver at a frequency of 4.7 MHz. (All materials described in this work were 6.3mm (0.25 in) thick). The symbols represent actual data points (peak heights of the echoes) and the solid curve is the predicted peak-height amplitude envelope considering birefringence only (eq. 4). Values for the attenuation ($a_1 = a_2 = .02$) were determined from data at $\theta = 0°$, $\phi = 0°$ and $\theta = 90°$, $\phi = 90°$. Birefingence data ($B_0 = 0.0036$) was obtained at the same angles. Figure 2b shows the same experimental data but the predicted curve is generated from eq. 7, with $G_3 = 0.2$ $a_3 = a_1$ and $f(\theta) = 0$, i.e., $k_3 = k_0$. A somewhat better fit is obtained using eq.7.

Similar results were observed for 7075-T651 aluminum. The experimental data is shown in Fig 3a along with the peak-height envelope predicted by eq. 4 and in Fig. 3b, with the curve generated

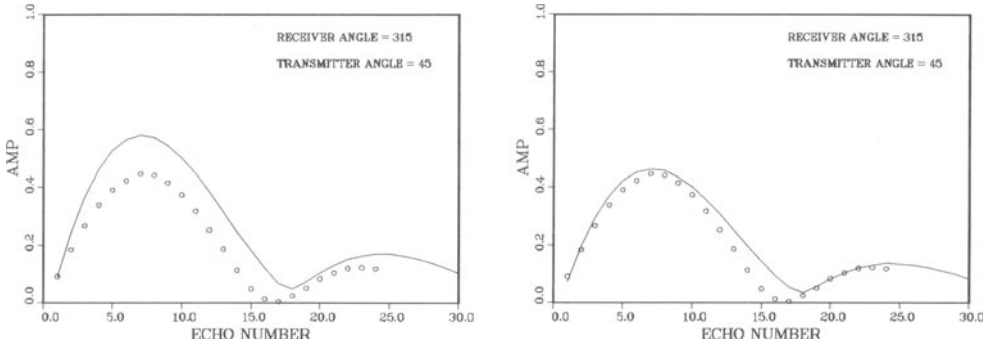

Fig. 2. Echo amplitude as a function of echo number for 2024-T351 aluminum using pitch-catch technique. Experimental data indicated by symbols. (a) Amplitude envelope calculated from eq. 4 shown as solid curve. (b) Amplitude envelope calculated from eq. 7.

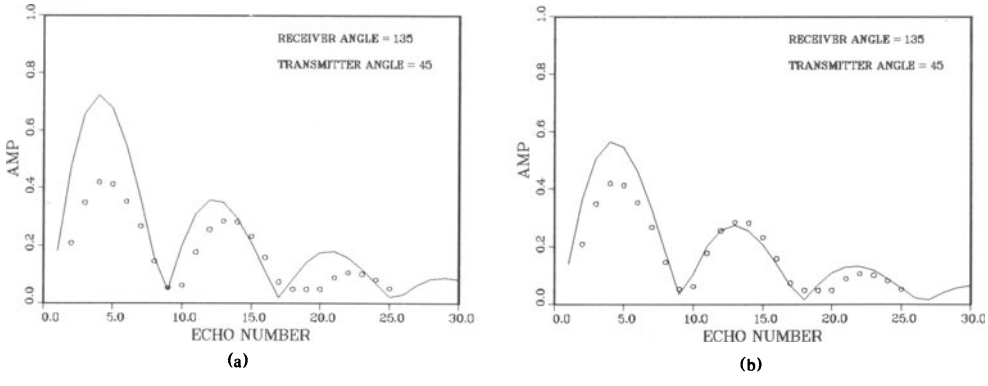

Fig. 3. Echo amplitude as a function of echo number for 7075-T651 aluminum using pitch-echo techniques. Experimental data indicated by symbols. (a) Amplitude envelope calculated from eq. 4 shown as solid curve. (b) Amplitude envelope calculated from eq. 7.

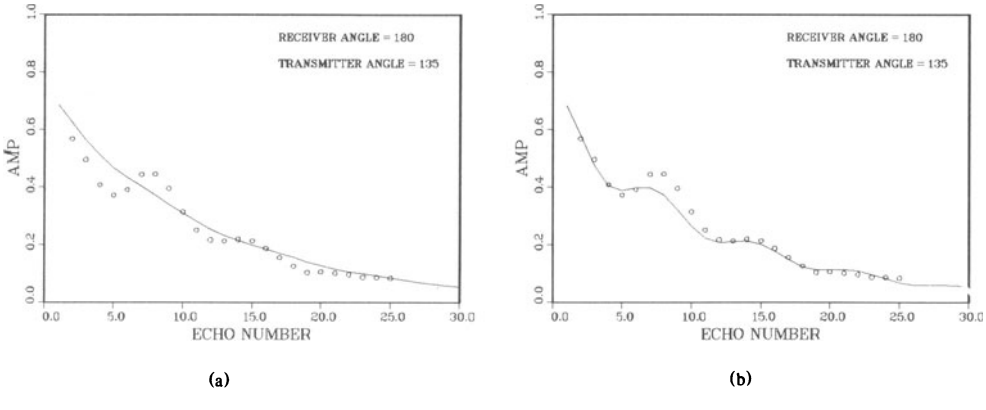

Fig. 4. Echo amplitude as a function of echo number for 7075-T651 aluminum using pitch-catch technique. Experimental data indicated by symbols. (a) Amplitude envelope calculated from eq. 4 shown as solid curve. (b) Amplitude envelope calculated from eq. 7.

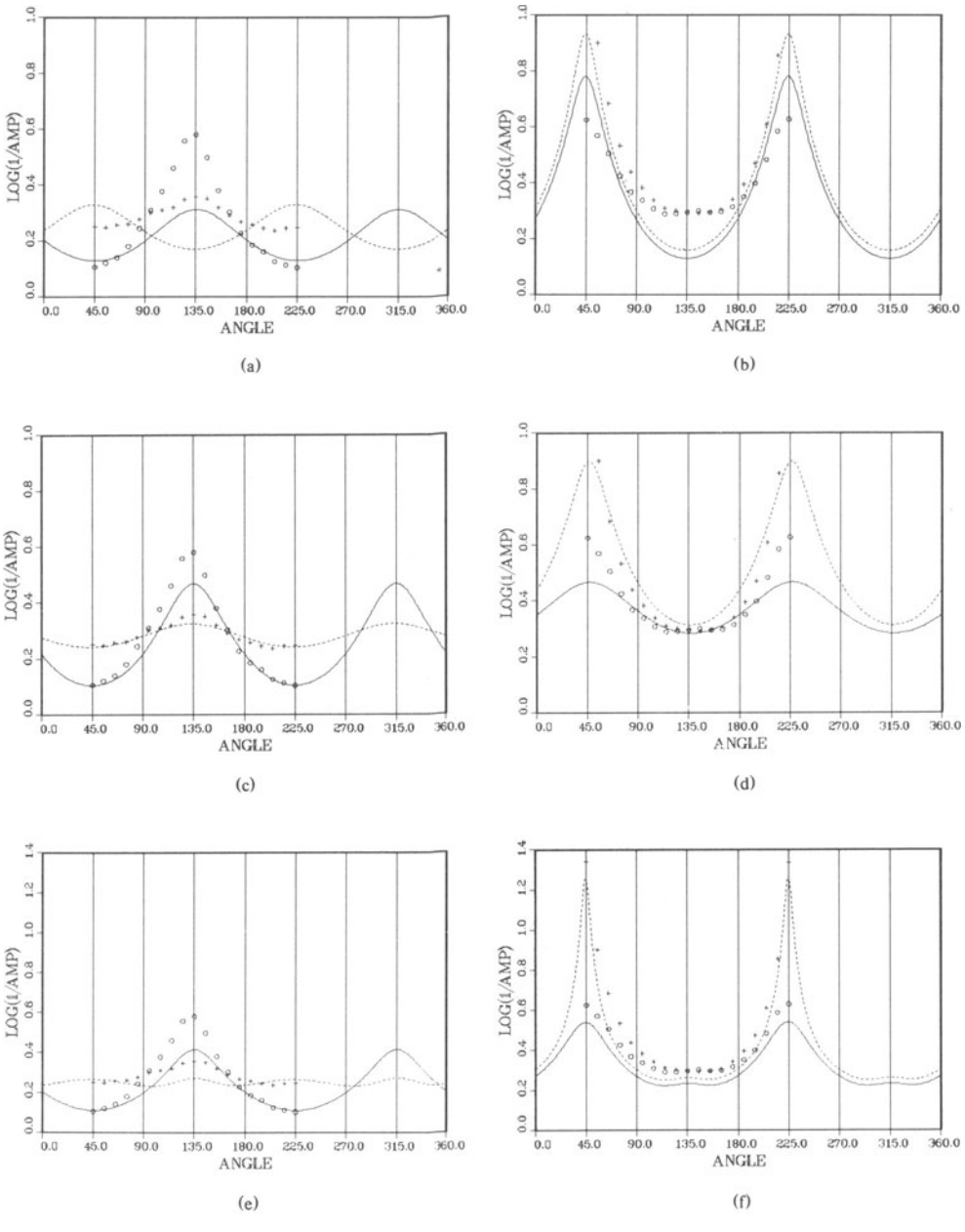

Fig. 5. Log of inverse echo amplitude versus receiver angle (transmitter angle, $\theta = 45°$) for 7075 aluminum specimen. (a) Experimental data shown as symbols, echo #2 as (o) and echo #3 as (+). Solid and dashed curve, echoes 2 and 3, respectively, computed from eq. 4. (b) Experimental data shown for echo #4 as (o) and echo #5 as (+). Solid and dashed curve, echoes 4 and 5, respectively, computed from eq. 7. (c) Same as (a) but using eq. 7. (d) Same as (b) but using eq. 7. (e) Same as (c) but using $f(\theta) = B_0 \cos 2\theta/2$ in eq. 7. (f) Same as (d) but using $f(\theta) = B_0 \cos 2\theta/2$ in eq. 7. (f).

from eq. 7, $f(\theta) = 0$. The birefringence of the 7075 aluminum was 0.0078 with $a_1 = 0.03$ and $a_2 = 0.035$ and the transducers polarizations were along $\theta = 45°$ and $\phi = 135°$. The better fit is again obtained with eq. 7. A second data set from the same specimen is shown in Fig. 4a and 4b with the transducers set at $\theta = 135°$ and $\phi = 180°$. As shown in Fig. 4a, eq. 4 predicts an exponential decay for $\phi = 180°$. However, the data displays a significant perturbation about the exponential decay. This deviation is 'reproduced' reasonably well by eq. 7, shown in Fig. 4b.

Figure 5a and 5b present amplitude data versus receiver polarization angle, ϕ, for the 7075 aluminum. Data are displayed as discrete points for echoes 2, 3, 4 and 5 over a range of receiver polarization angles of $\phi = 45°$ through $\phi = 225°$ and transmitter polarization angle of $\theta = 45°$. The curves are those predicted by eq. 4 for the same echo numbers over a range of $\phi = 0°$ to $\phi = 360°$. As shown in Fig. 5a, eq. 4 predicts a local amplitude minimum at $\phi = 45°$ whereas the data displays a local maximum. Figure 5c and 5d present the same data along with curves predicted by eq. 7, $G_3 = 0.3$. The local minima and maxima agree for all of the echo numbers. Upon close examination of the data for echoes 4 and 5, a 'weak' maximum is observed to occur for $\phi \approx 145°$. If $f(\theta) = (B \cos 2\theta)/2$ and $G_3 = 0.21$ in eq. 7, the generated curves have a weak maximum at $\phi = 135°$, shown in Fig. 5f. In general, for all of the data presented, numerical curve fitting over a number of parameters would be necessary to improve the agreement.

DISCUSSION

The purpose of this paper has been to present bulk-wave ultrasonic measurements that may be indicative of texture inhomogeneities through the thickness of rolled plates, i. e. a layered structure or possible coherent 'scattering'. Equation 4 was used to predict the effects of birefringence on normal incidence SH-waves considering the resultant splitting of the waves to have polarizations parallel to the X_1 and X_2 directions. Equation 7 was introduced as an attempt to better fit the experimental data. The extra term in eq. 7 which accounts for a secondary splitting of the wave is quite similar to the additional term used by Truell, Elbaum and Chick[5] to account for lack of parallelism. This additional term may or may not be physically correct, but it does seem to reproduce many of the features displayed by the data. Consideration is currently being given to a derivation based upon a smoothly varying, symmetric layered texture and numerical curve-fitting of the data.

ACKNOWLEDGMENT

The authors would like to thank H. H. Chaskelis for many useful discussions. This work was supported by the Office of Naval Research.

REFERENCES

1. E. P. Papadakis, IEEE Trans. Sonics Ultrason. 11, 19 (1964).

2. A. V. Clark and R. B. Mignogna, Ultrasonics 21, 57 (1983).

3. R. B. Mignogna, A. V. Clark, B. B. Rath, and C. L. Vold, in Nondestructive Methods for Material Property Determination, C. Olaf and R. E. Green, Jr., Eds. (Plenum Press, New York, 1984), p. 339.

4. Y. Iwashimizu and K. Kubomura, Int. J. Solids Struct. 9, 99 (1973)

5. R. Truell, C. Elbaum and B. B. Chick, "Ultrasonic Methods in Solid State Physics," (Academic Press, New York and London, 1969).